Defect formation during powder compaction

William Zunker, Sachith Dunatunga, Subhash Thakur,
Pingjun Tang, Ken Kamrin
Department of Mechanical Engineering, Massachusetts Institute of Technology
Department of Mechanical Engineering, University of California Berkeley
Vertex Pharmaceuticals

2025 IFPRI Annual General Meeting
Marseille, France

IFPRI MITMECHE Berkeley Department of Mechanical Engineering COLLEGE OF ENGINEERING VERTEX LAMMPS

CXM
丞祥机械
www.chinapillpress.com

Capping

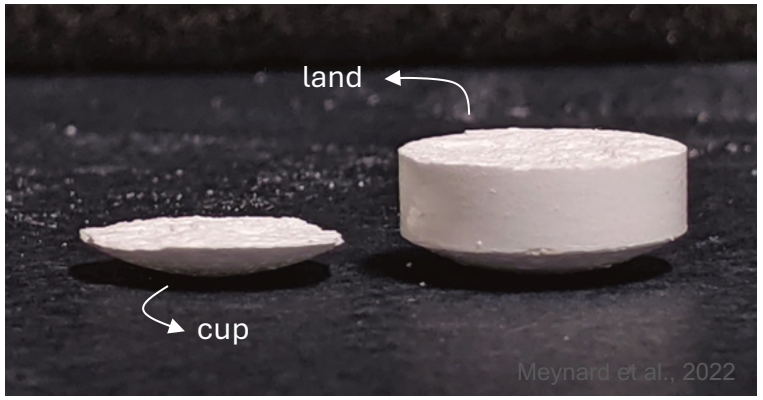

- Primarily observed in bi-convex tablets: splitting of one or both cups.

- Combined effects:

  - Mode II shear stress failure at interface between cup and land.
  - Entrapped air.

Lamination

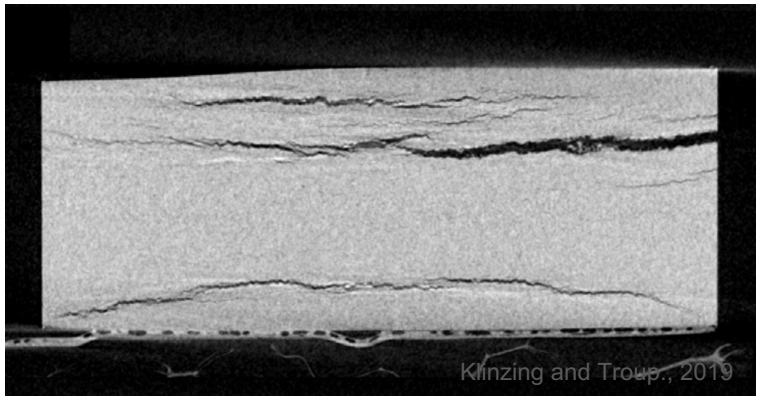

- Type I: Multiple fracture caused by air entrapment.

  - Caused by high-speed compression and high relative density.
  - More common in ductile materials.
  - Fracture pattern is random.

- Type II: Shear stresses combined with radial expansion during ejection.

  - Occurs more often with less lubrication.
  - Reproducible fracture at bottom of tablet.
  - Less common in ductile materials.

Continuum methods

Homogenize powder into continuous media

\+ arbitrarily large system sizes

− no accepted cohesive powder constitutive model

− no particle-level details

Discrete element method

Discretely represent powders as primitive spheres

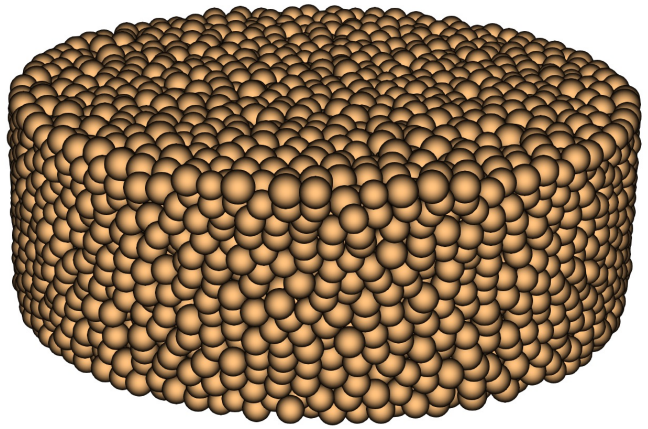

\+ computational efficiency between continuum & MPFEM

\+ particle-level details

\+ pore-level gas phase coupling possible

MPFEM

Discretely represent powders as meshed continuum bodies

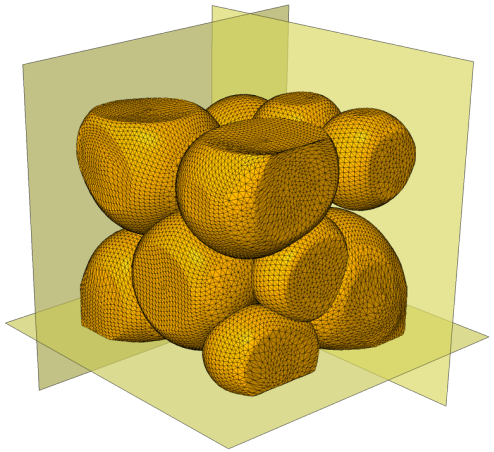

\+ complex shapes and multi-material interactions

\+ particle-level details

− computational expense

Powders are complex:

- Elastic
- Plastic
- Viscoelastic
- Adhesion
- Liquid bridging
- Friction
- Fracture
- Triboelectric charging
- Sintering
- Segregation
- Multi-component blends

Method of dimensionality reduction (MDR) contact model

- Analytical mechanics-based formulation
- Physical model inputs: $E, \nu, Y, \Delta\gamma$
- Models elasto-plastic behavior into high confinement and during unloading
- Includes JKR type (fracture) adhesion
- Formally implemented into main LAMMPS repository: LAMMPS

MPFEM

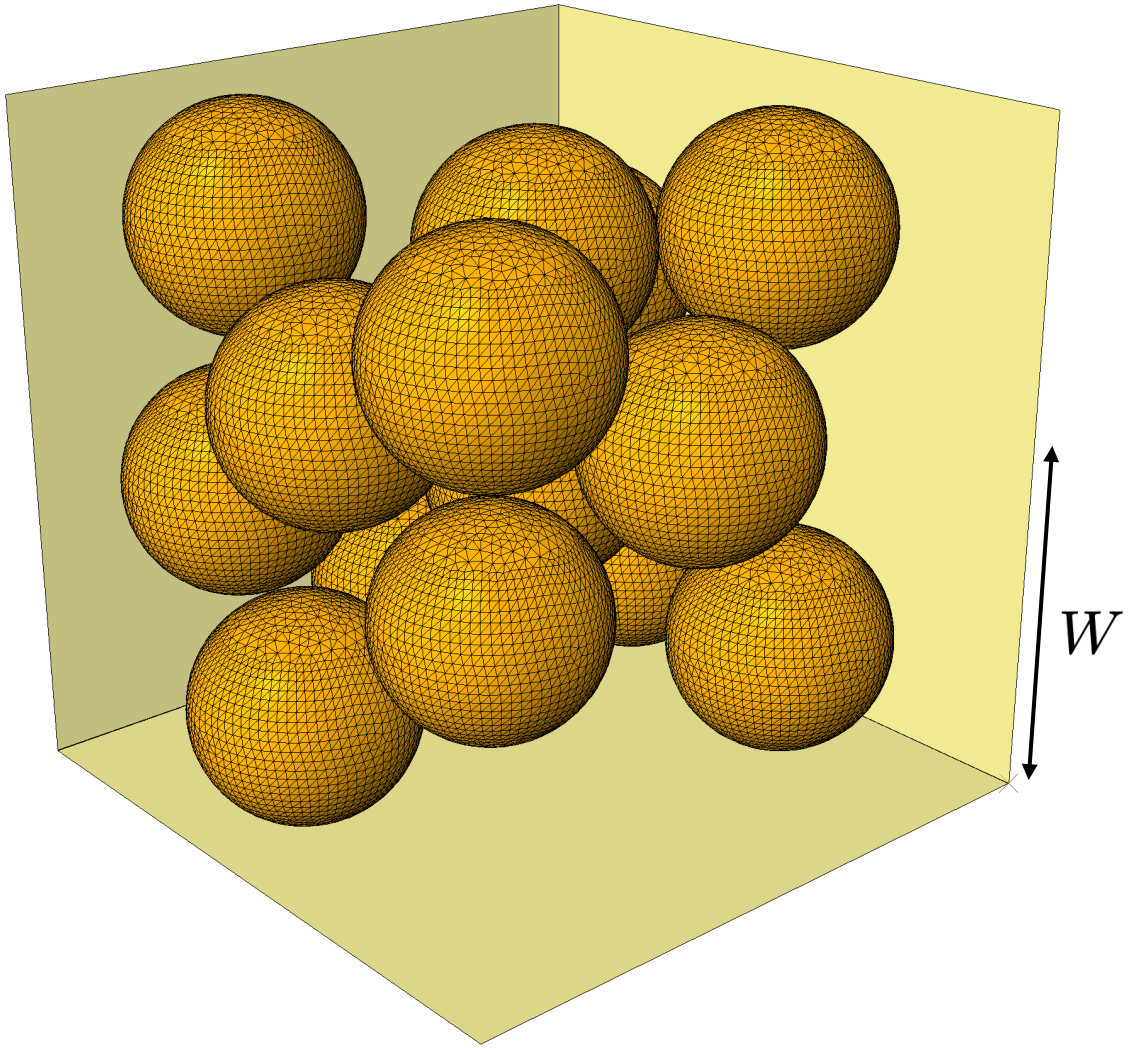

undeformed

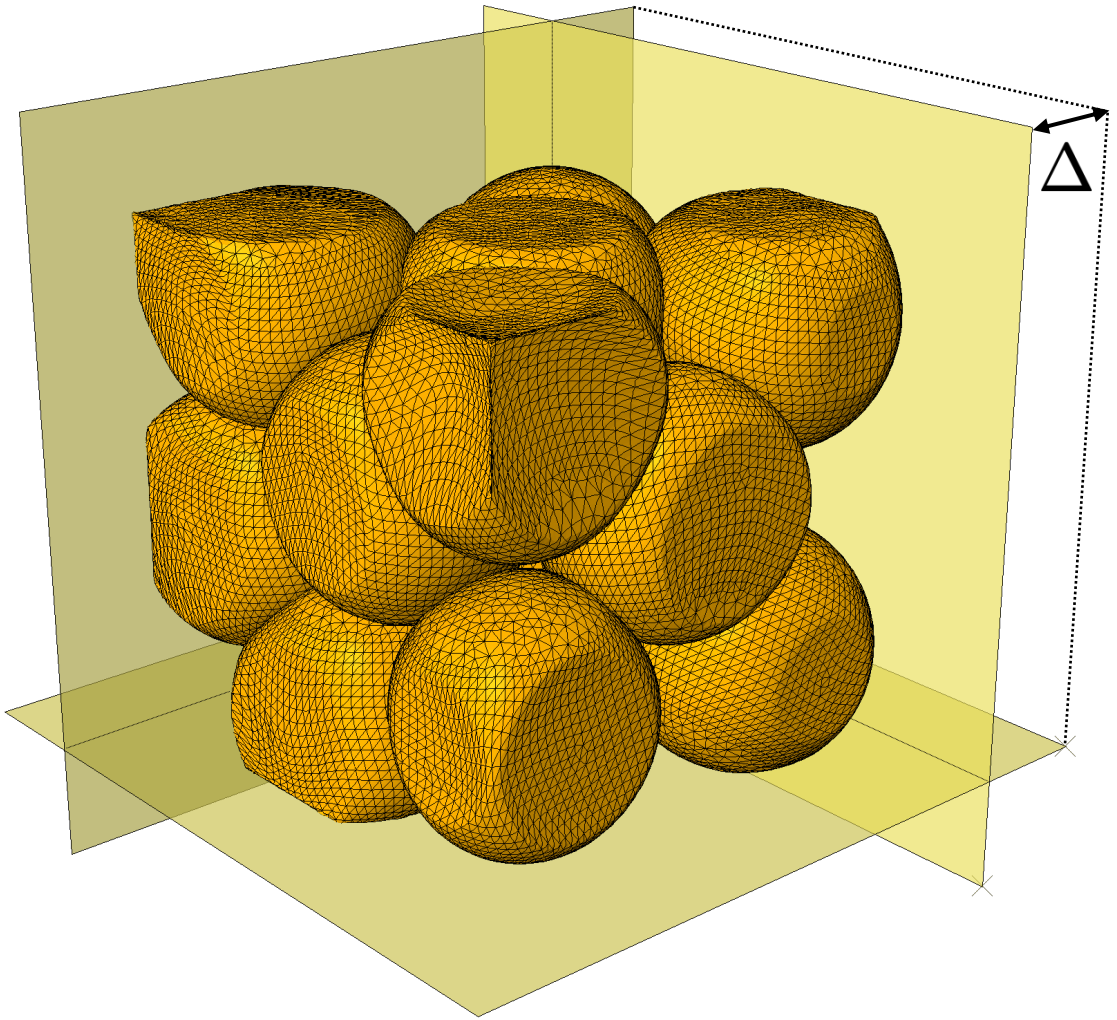

deformed

monodisperse

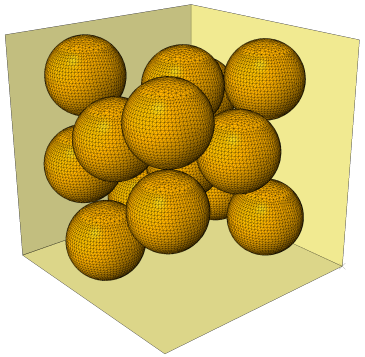

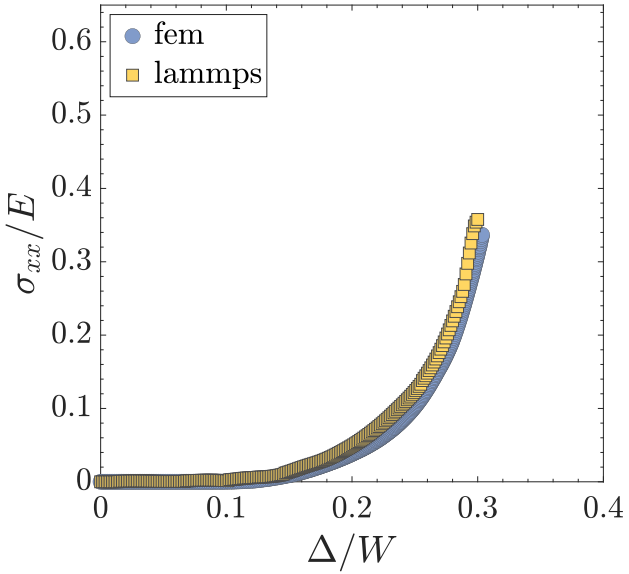

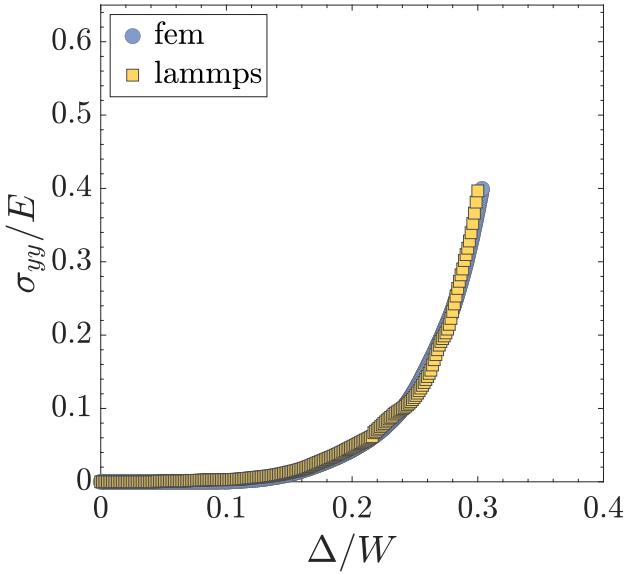

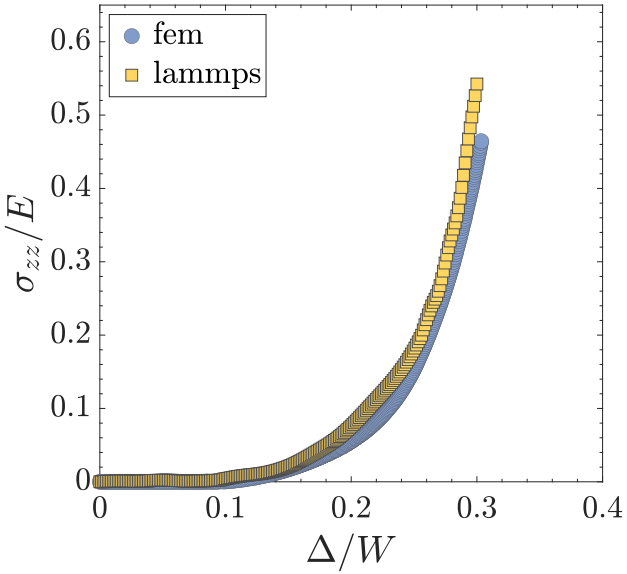

tridisperse

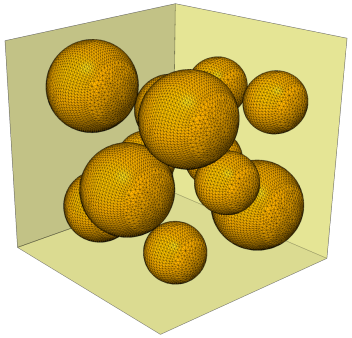

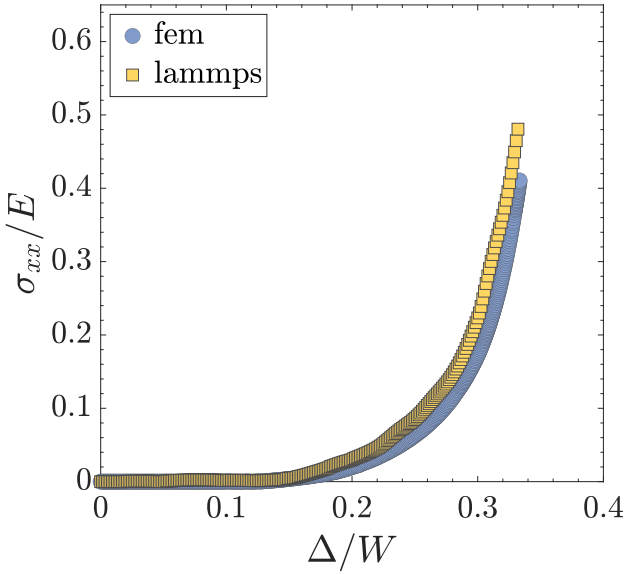

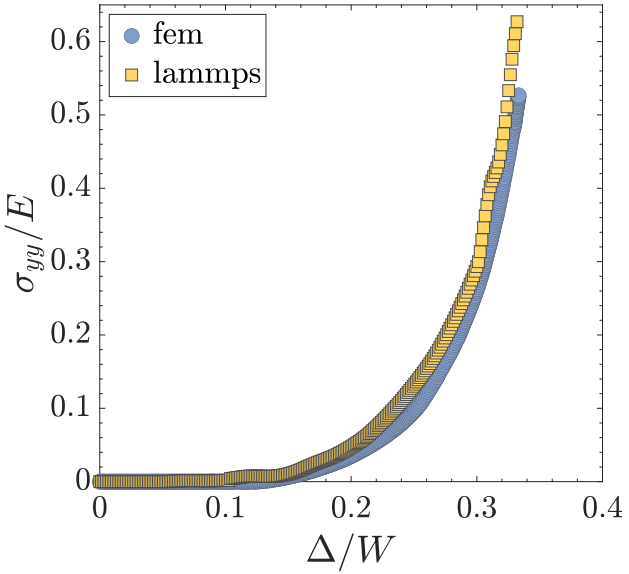

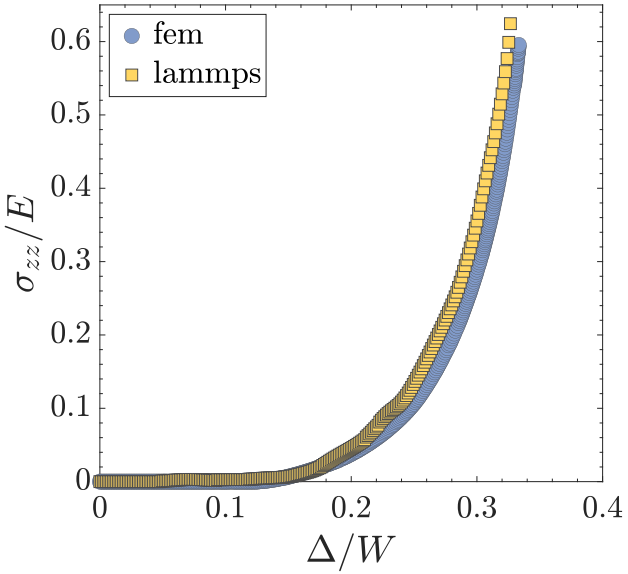

Particle Reconstruction

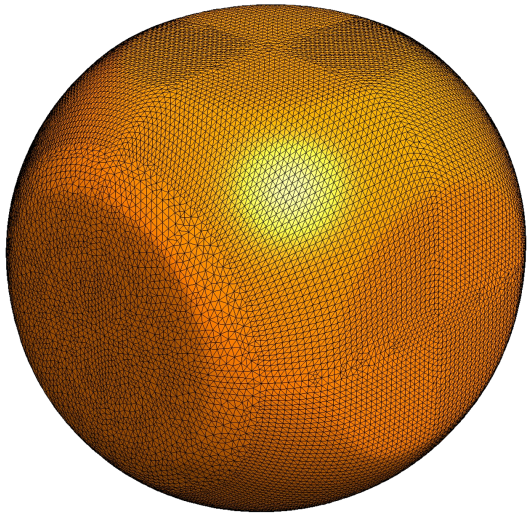

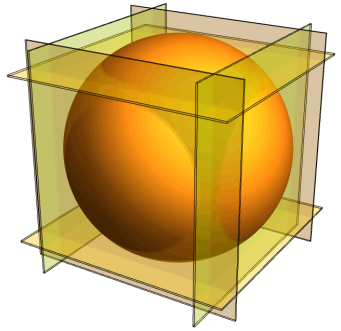

triaxial compaction

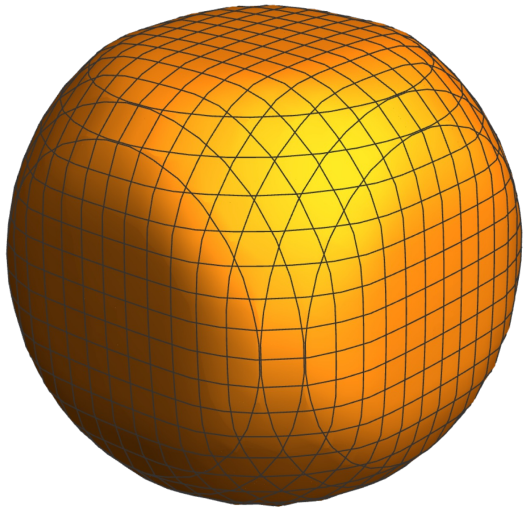

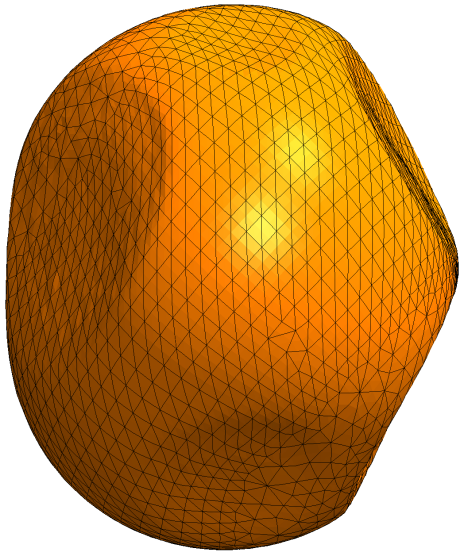

finite element

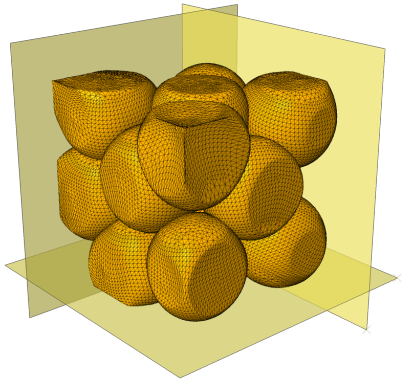

monodisperse MPFEM

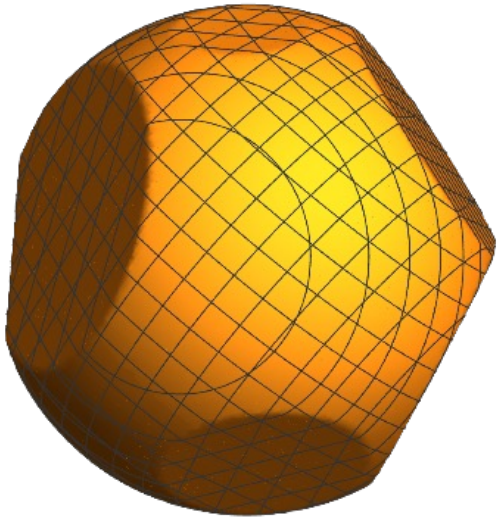

MDR contact model

Experimental Compaction Simulator

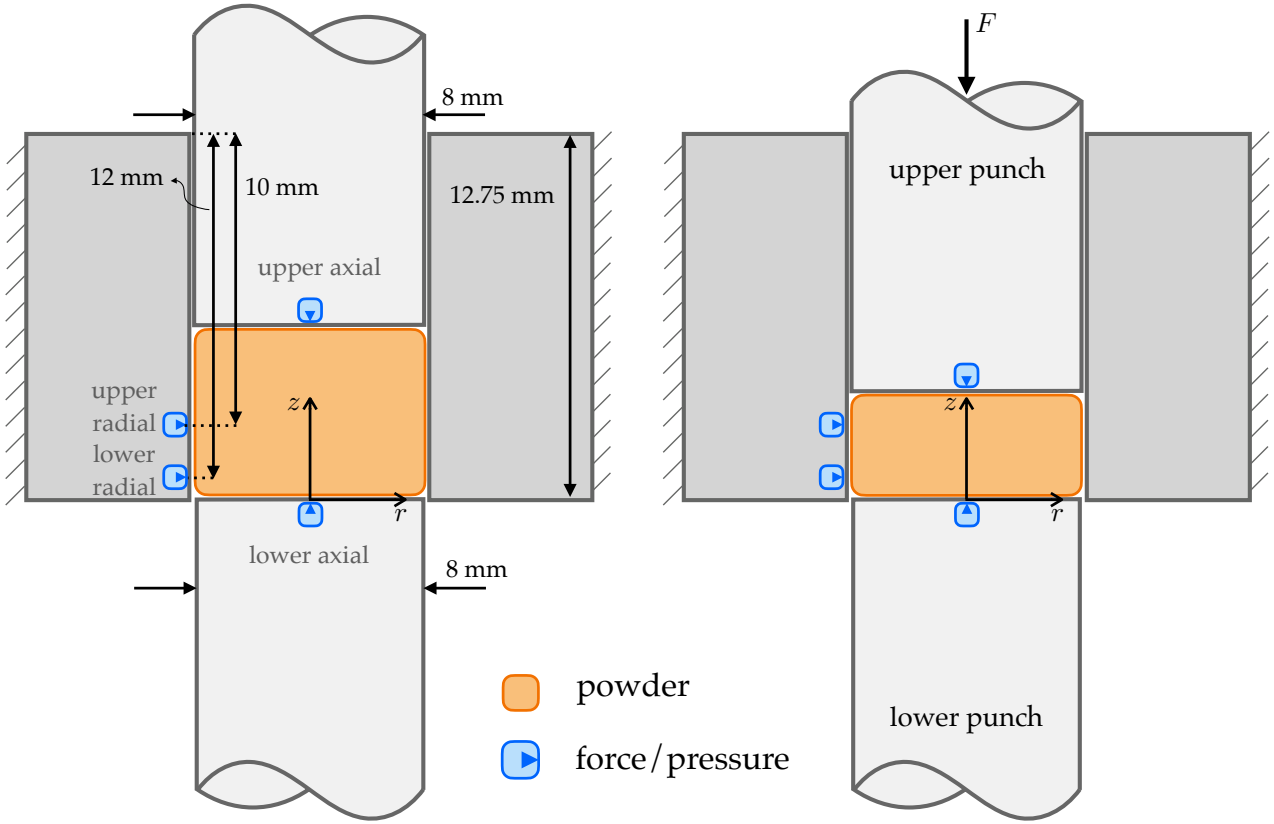

Avicel PH102

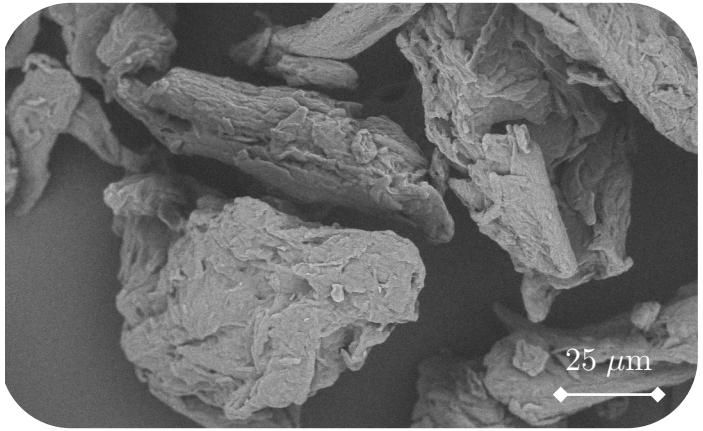

Calibrated DEM Parameters

Normal (MDR)	**Tangential (LH)**
$E = 8\,\text{GPa}$	$k_t = \frac{2}{7}ER_{\text{mean}}\,\text{N/m}$
$\nu = 0.3$	$x_{\gamma,t} = 1.0$
$Y = 77\,\text{MPa}$	$\mu_t = 0.3$
$\Delta\gamma = 900\,\text{J/m}^2$	$\mu_{t,\text{wall}} = 0.1$
$\psi_b = 0.125$	
$\eta_n = 1e4\rho R_{\text{mean}}^2 v_p\,\text{kg/s}$	
Rolling (SDS)	**Particle**
$k_{\text{roll}} = \frac{9}{4}\mu_{\text{roll}}^2 ER_{\text{mean}}\ \text{N/m}$	$R_{\text{min}} = 139\,\mu\text{m}$
$\gamma_{\text{roll}} = \eta_n$	$R_{\text{max}} = 160\,\mu\text{m}$
$\mu_{\text{roll}} = 1.0$	$\rho = 1560\,\text{kg/m}^3$

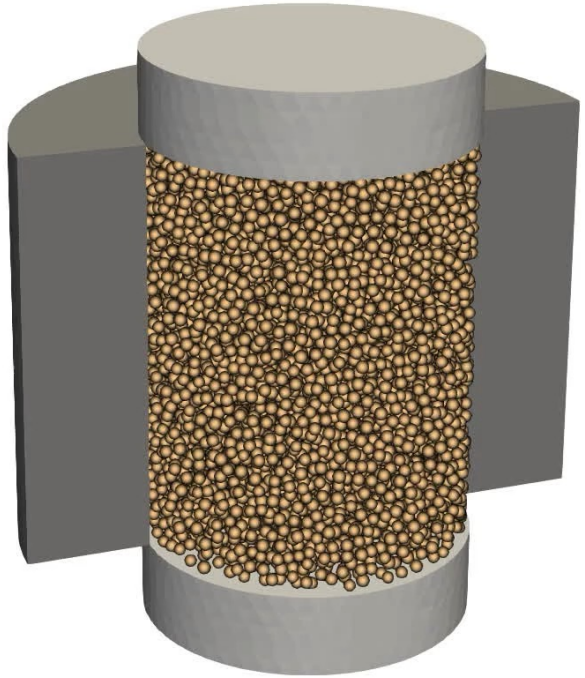

$RD_{max} = 0.85$

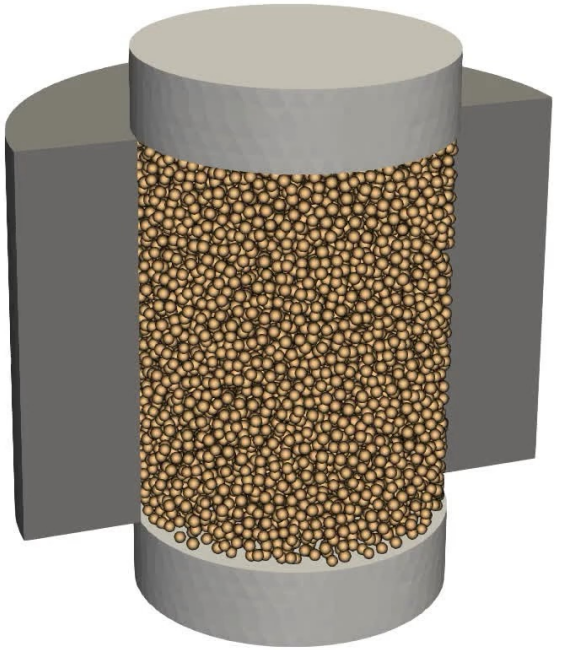

$RD_{max} = 0.99$

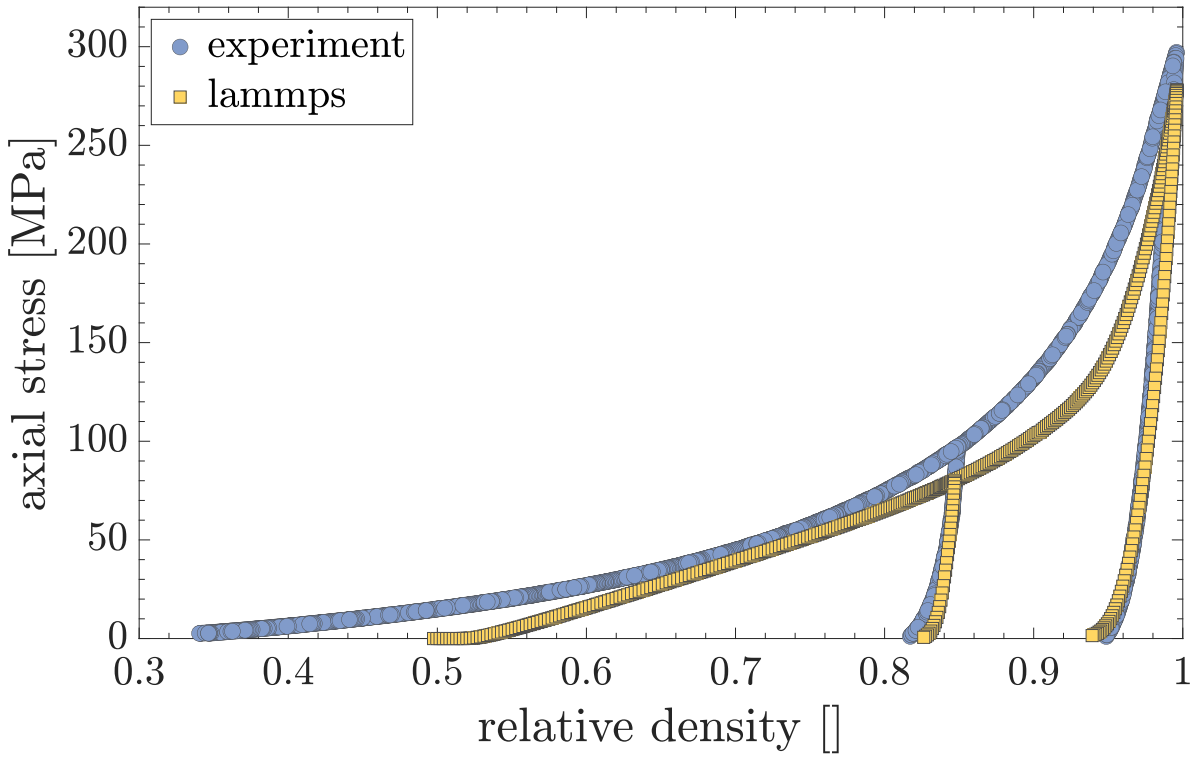
experiment
lammps
axial stress [MPa]
relative density []
0
50
100
150
200
250
300
0.3
0.4
0.5
0.6
0.7
0.8
0.9
1

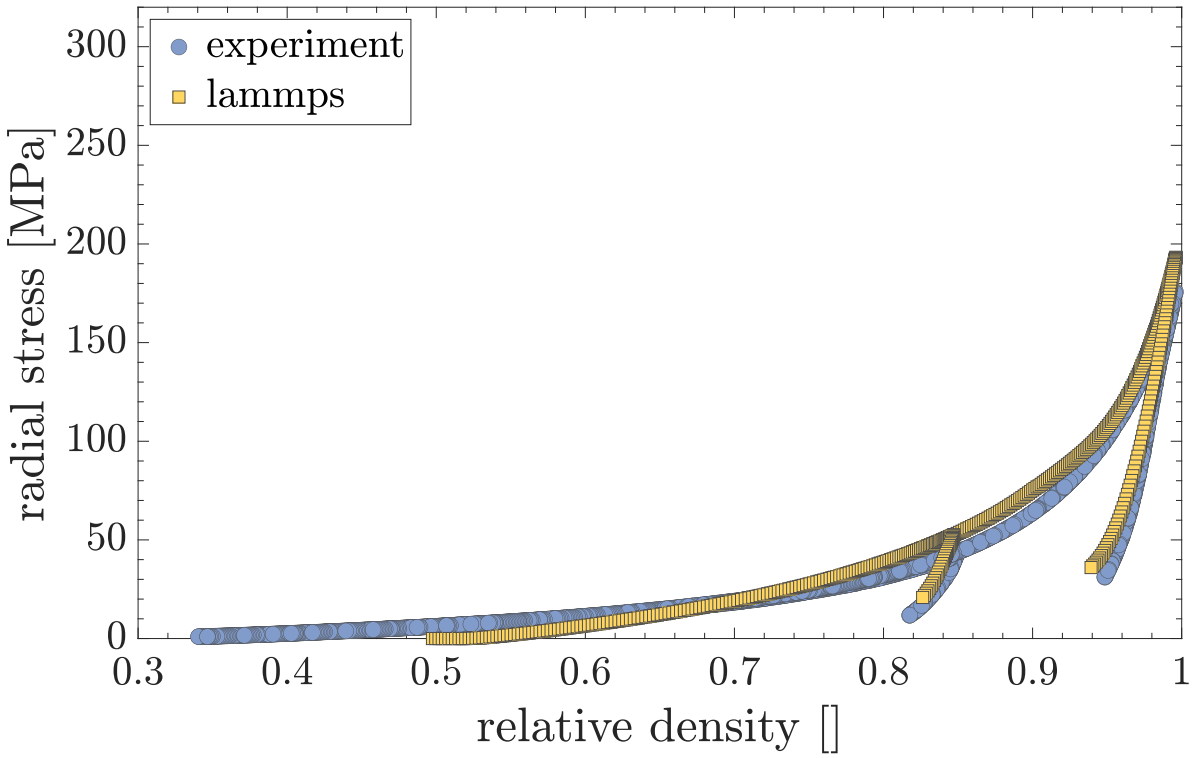
experiment
lammps
radial stress [MPa]
relative density []
0
50
100
150
200
250
300
0.3
0.4
0.5
0.6
0.7
0.8
0.9
1

Beyond Tableting…

Pieter’s Pelleting Process

Publications and Code

- Zunker, W., & Kamrin, K. (2024). A mechanically-derived contact model for adhesive elastic-perfectly plastic particles, Part I: Utilizing the method of dimensionality reduction. *Journal of the Mechanics and Physics of Solids*, *183*, 105492.

- Zunker, W., & Kamrin, K. (2024). A mechanically-derived contact model for adhesive elastic-perfectly plastic particles, Part II: Contact under high compaction—modeling a bulk elastic response. *Journal of the Mechanics and Physics of Solids*, *183*, 105493.

- Zunker, W., Dunatunga, S., Thakur, S., Tang, P., & Kamrin, K. (2025). Experimentally validated DEM for large deformation powder compaction: Mechanically-derived contact model and screening of non-physical contacts. *Powder Technology*, *459*, 120972.

LAMMPS Github

MDR Contact Model Documentation

Published in April!

Powder Technology 459 (2025) 120972

Contents lists available at ScienceDirect

Powder Technology

journal homepage: www.journals.elsevier.com/powder-technology

Experimentally validated DEM for large deformation powder compaction: Mechanically-derived contact model and screening of non-physical contacts

William Zunker [a], Sachith Dunatunga [a], Subhash Thakur [c], Pingjun Tang [c], Ken Kamrin [a,b,*]

[a] Department of Mechanical Engineering, Massachusetts Institute of Technology, 77 Massachusetts Ave, Cambridge, 02319, MA, USA
[b] Department of Mechanical Engineering, University of California Berkeley, University Ave, Berkeley, 94720, CA, USA
[c] Vertex Pharmaceuticals, 50 Northern Avenue, Boston, 02210, MA, USA

HIGHLIGHTS

- Large deformation adhesive elastic–plastic powder compaction is studied.
- A recently proposed adhesive elastic–plastic contact model is further developed.
- A new algorithm screens non-physical contacts in large deformation DEM simulations.
- The extended contact model is implemented in LAMMPS and validated with MPFEM.
- Pharmaceutical tableting simulations show strong agreement with experimental data.

GRAPHICAL ABSTRACT

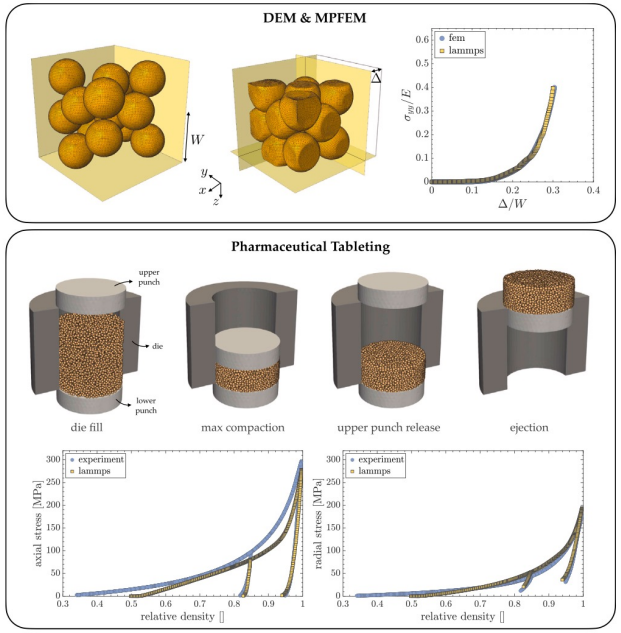

Adding in air…

Multi-particle collision dynamics (MPCD or SRD)

Models a compressible fluid as a collection of point-like particles that follow simplified dynamics in three steps:

1. Streaming – propagates momentum

$$\mathbf{x}_i(t + \Delta t) = \mathbf{x}_i(t) + \mathbf{v}_i(t)\Delta t$$

2. Bounce-Back – MPCD particles reflect off DEM particles and momentum is exchanged.

3. Collision – momentum exchange per cell

$$\mathbf{v}_{\mathrm{cm}} = \frac{1}{N_c}\sum_{i=1}^{N_c}\mathbf{v}_i$$

$$\mathbf{v}_i = \mathbf{v}_{\mathrm{cm}} + \mathbf{R}(\mathbf{v}_i - \mathbf{v}_{\mathrm{cm}})$$

✚ Recovers compressibility and viscosity
✚ Existing LAMMPS MPCD-DEM coupling

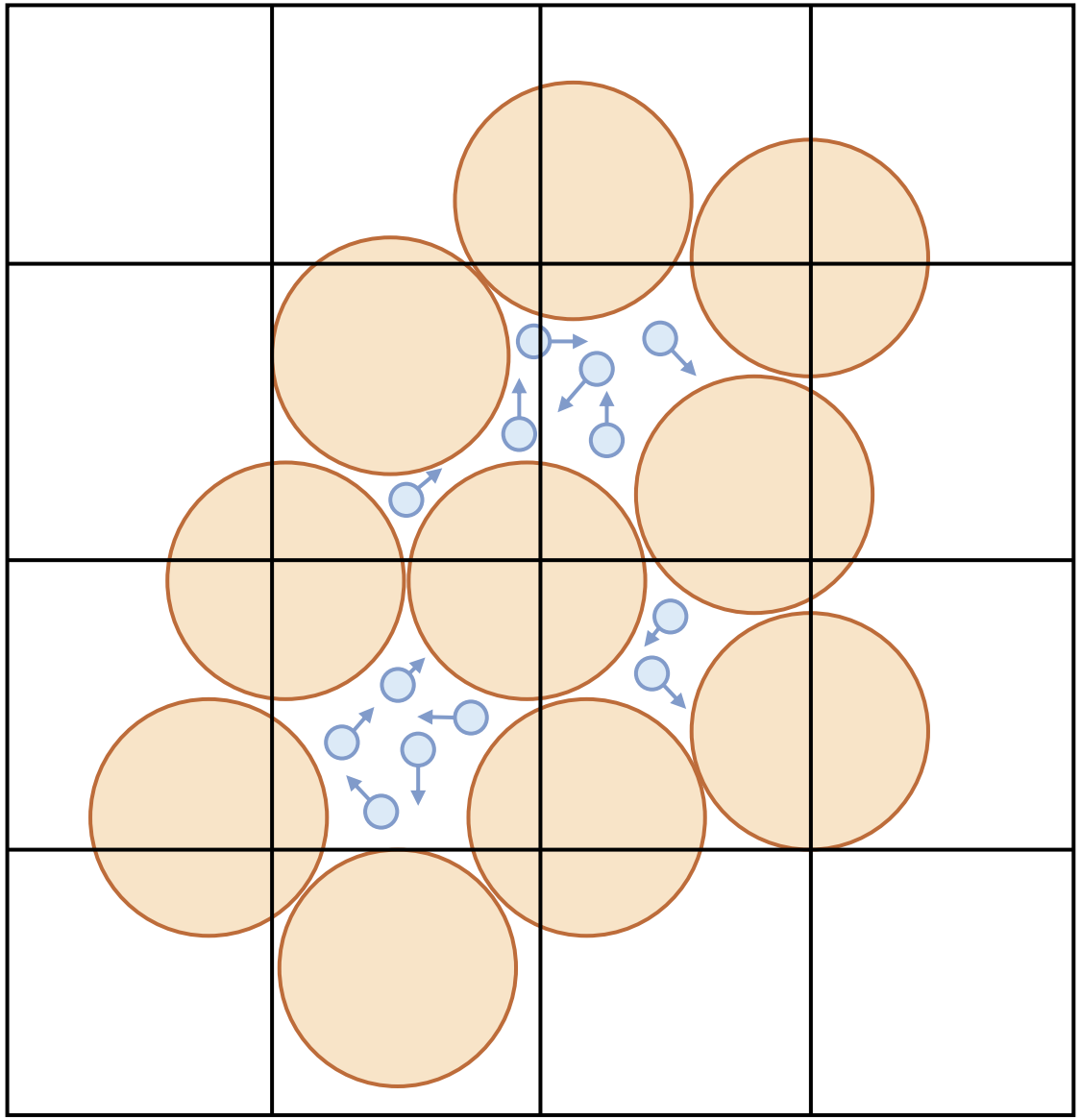

= DEM = MPCD

Air-Induced Defect Study

reference simulations

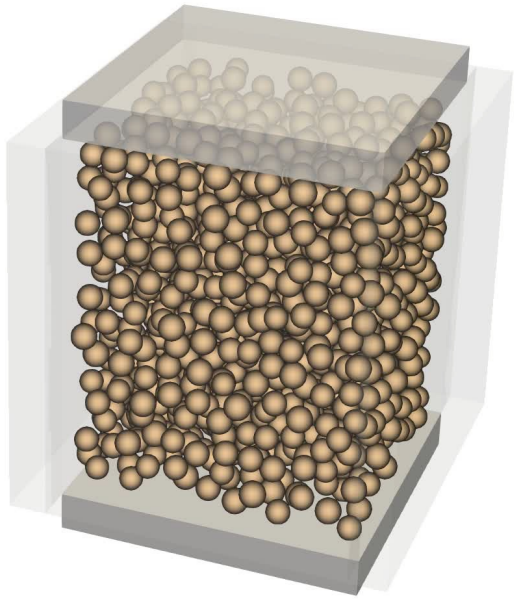

no air

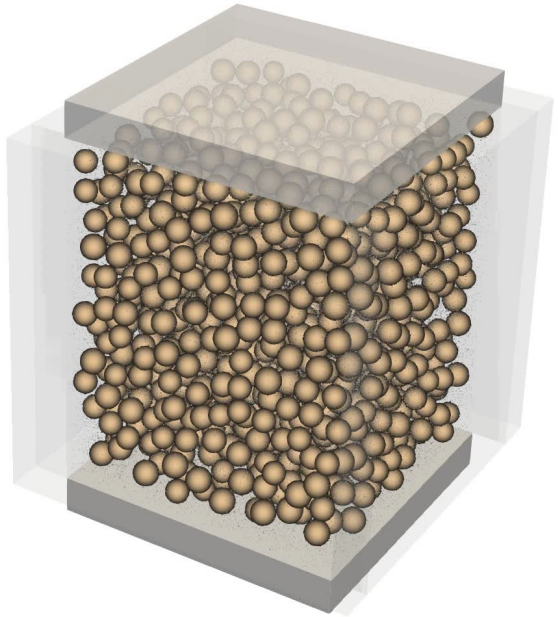

with air

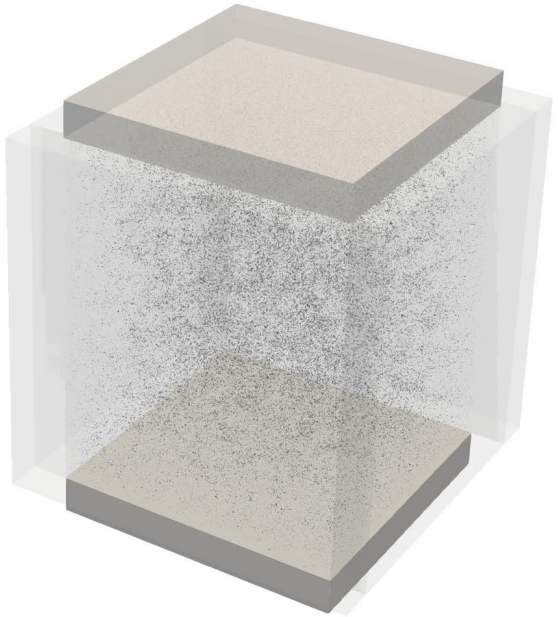

with air (DEM hidden)

Air-Induced Defect Study

10x increased air viscosity

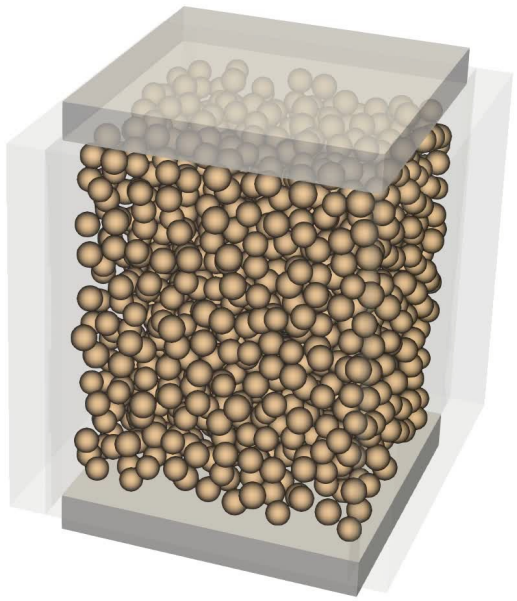

no air

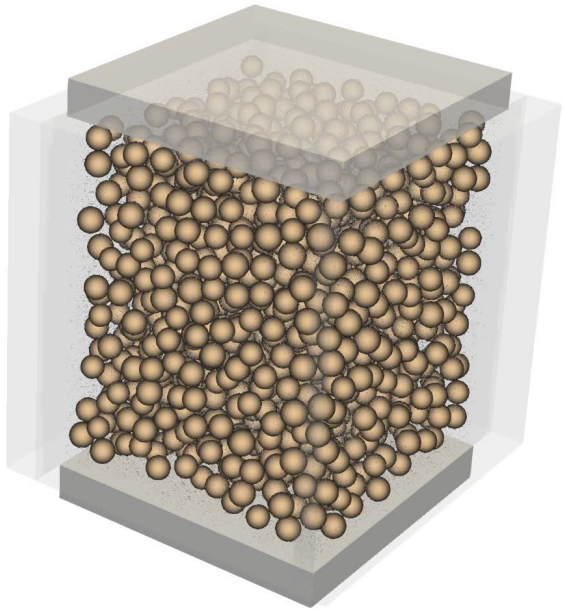

with air

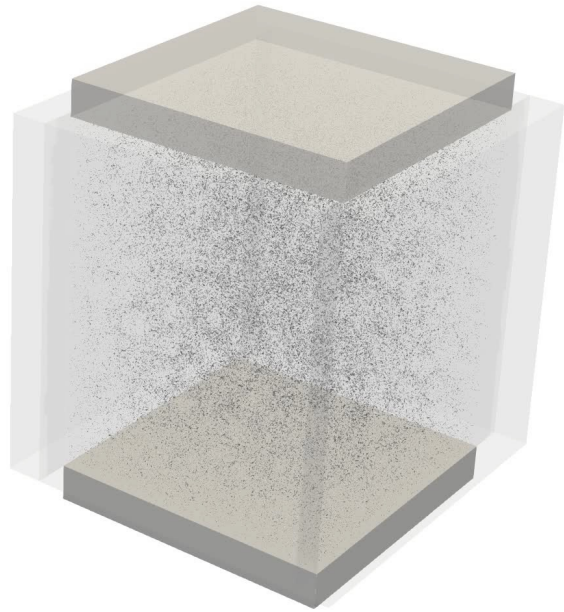

with air (DEM hidden)

Air-Induced Defect Study

10x increased air viscosity and reduce maximum relative density (0.98 → 0.9)

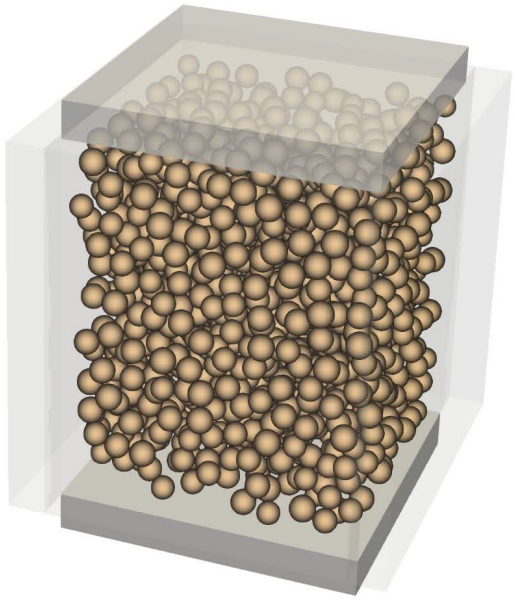

no air

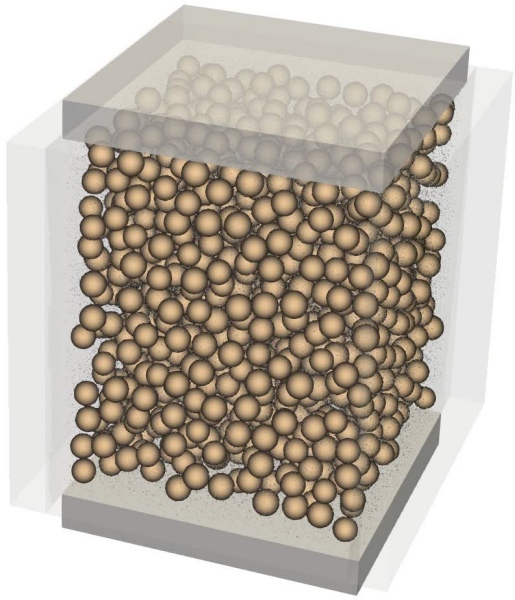

with air

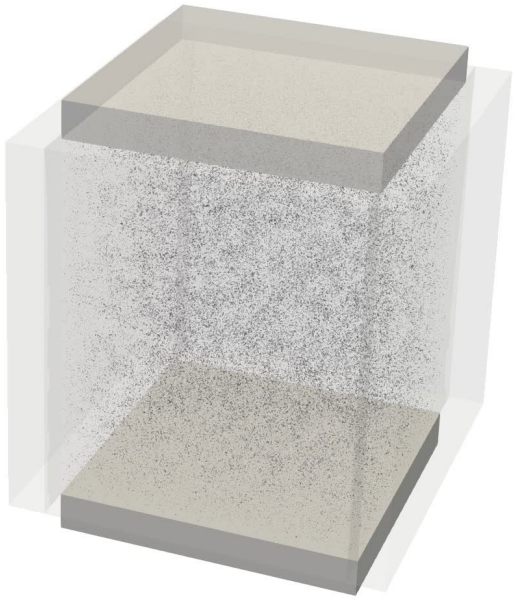

with air (DEM hidden)

Final Formed Tablets with Air

laminar defects observed

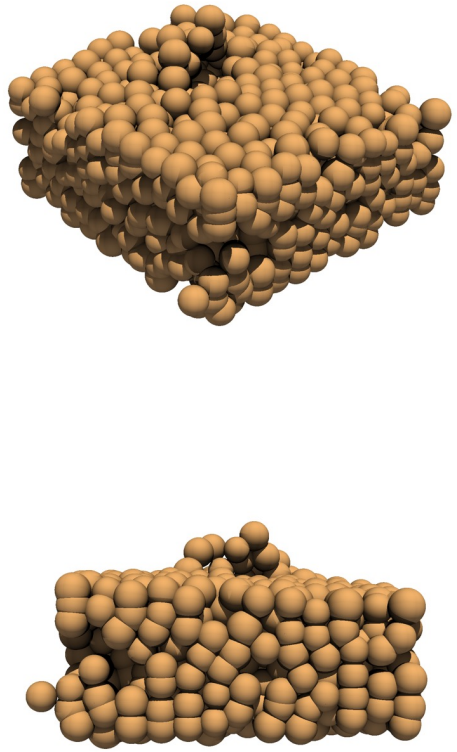

reference

laminar defects observed

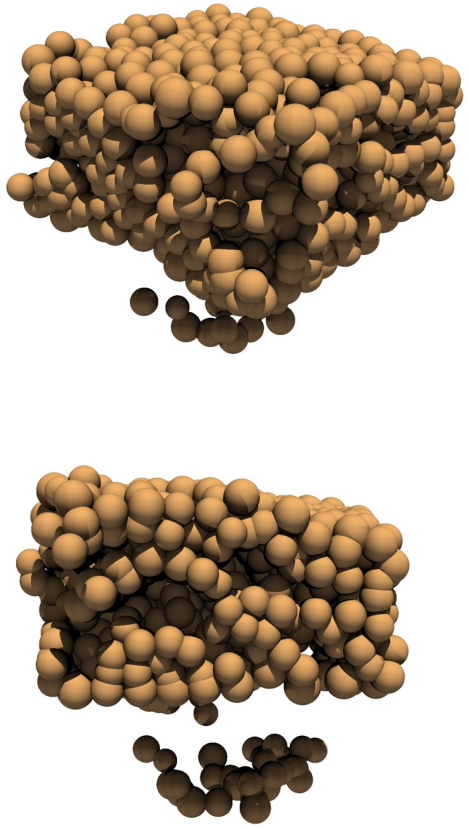

10x increased air viscosity

no defects observed

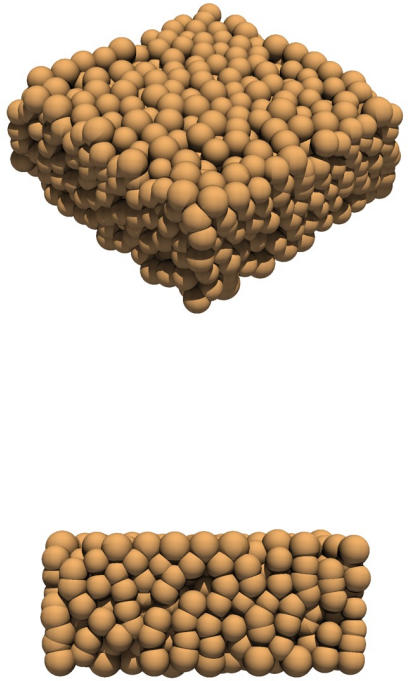

10x increased air viscosity and reduce maximum relative density from (0.98 → 0.9)

Curious follow-up… Sticking

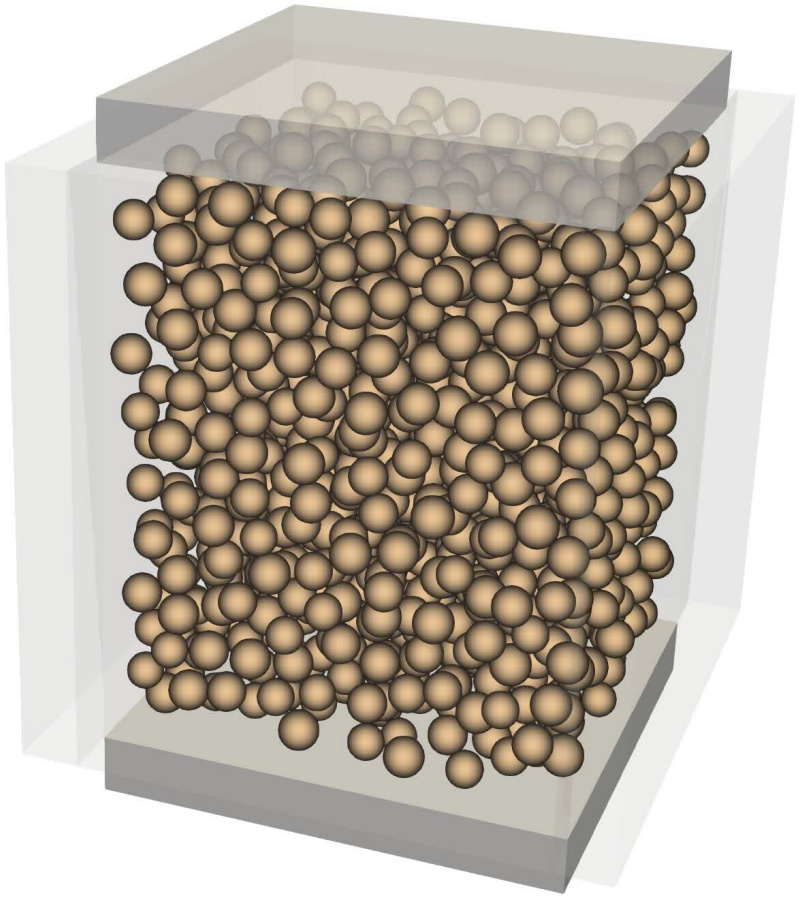

no air

$\Delta\gamma_{\mathrm{wall}}/\Delta\gamma$ = 1/3

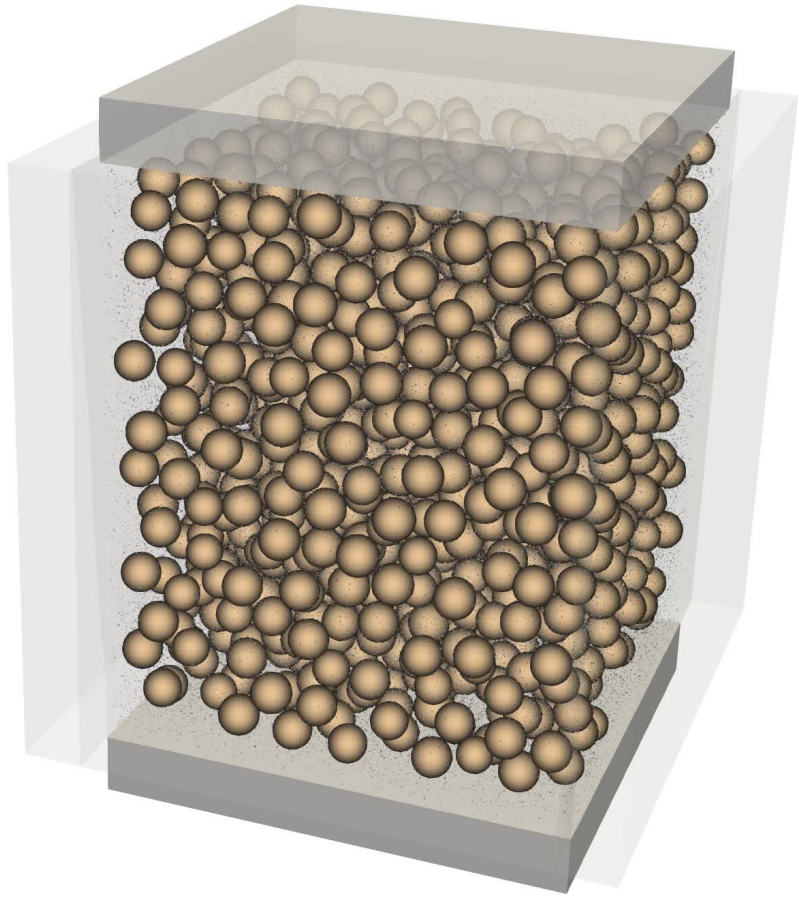

with air

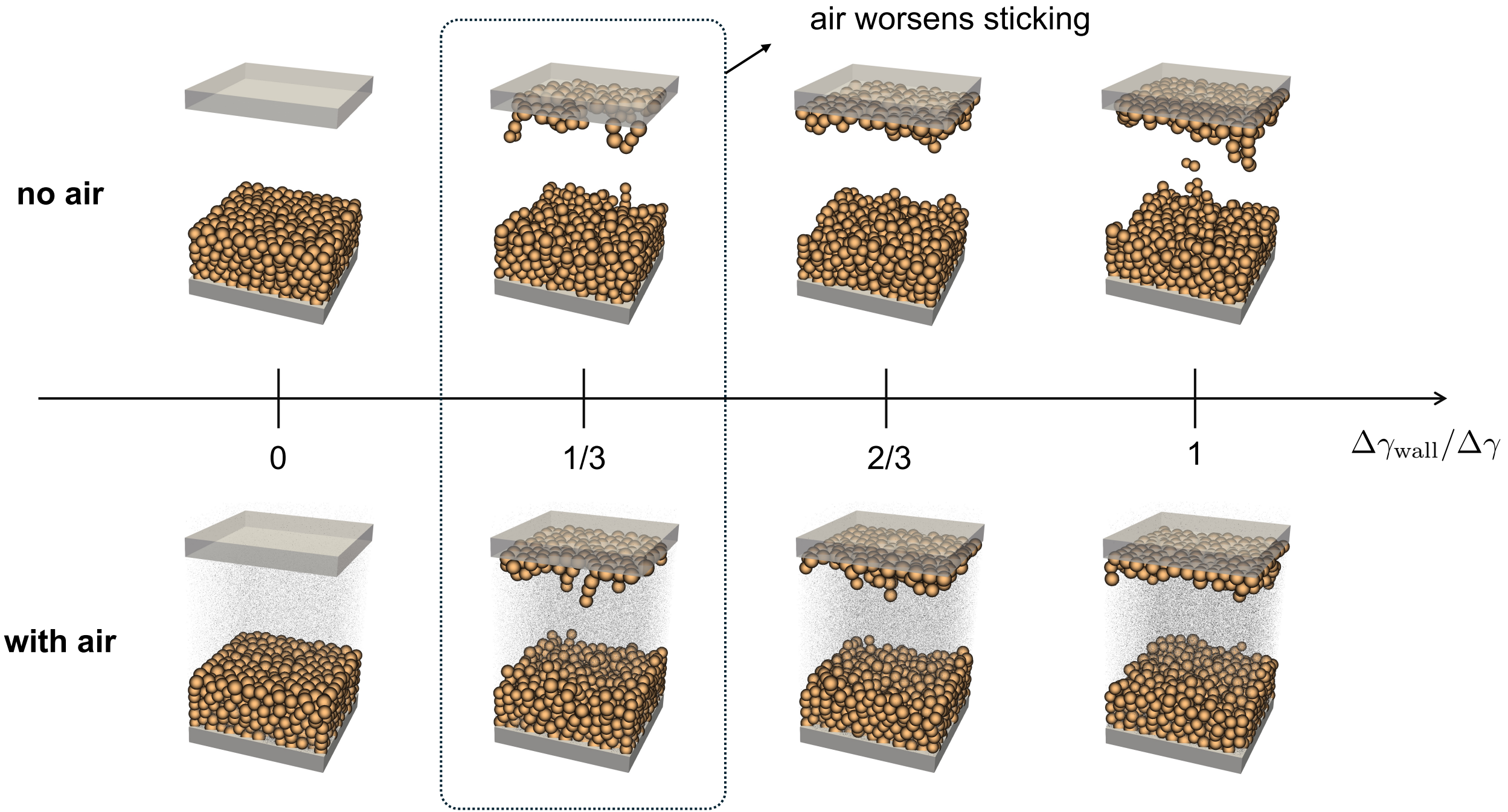
air worsens sticking
no air
with air
0
1/3
2/3
1
$\Delta\gamma_{\mathrm{wall}}/\Delta\gamma$

Overall Summary of Project Progress

- Developed a novel mechanically-derived contact model for adhesive elastic-perfectly plastic particles.

- Published two papers in JMPS on the theory of the model.

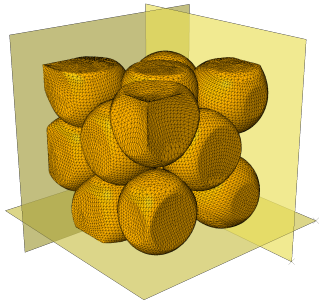

- Formally implemented the contact model and a new topological algorithm into the main repository of the open-source software LAMMPS.

- Validated the code against FEM and experimental results in collaboration with Vertex Pharmaceuticals.

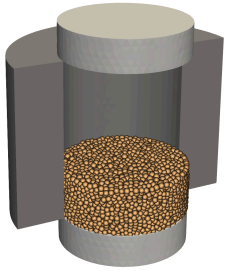

- Published a paper in Powder Technology highlighting the LAMMPS code and its practical application in modeling powder compaction.

- IFPRI members (Pieter and Amir) and others are using the model to simulate a wide array of powder compaction applications from pelleting to battery calendaring.

- Worked to achieve coupling with a compressible gas phase in LAMMPS.

- Demonstrated the sticking defect and the role of air in worsening the effect.

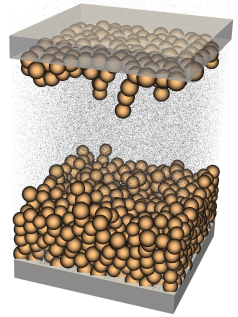

- Produced air-induced lamination defects with simulation using the DEM representation of Avicel under reasonable operating conditions.

- Showed that the lamination defects are sensitive to air viscosity (i.e. loading rates) and maximum relative density, consistent with literature findings.

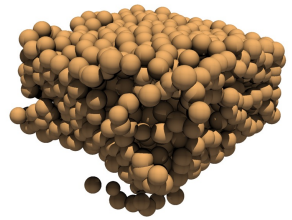

Appendix

Lamination

Mazel and Tchoreloff, 2021

- MCC lamination defects observed under the following conditions:

- 80 mm/s punch velocity
- 230 MPa maximum axial stress
- Straight and tapered die
- Precompressions less than 20 MPa and greater than 130 MPa

Klinzing and Troup, 2019

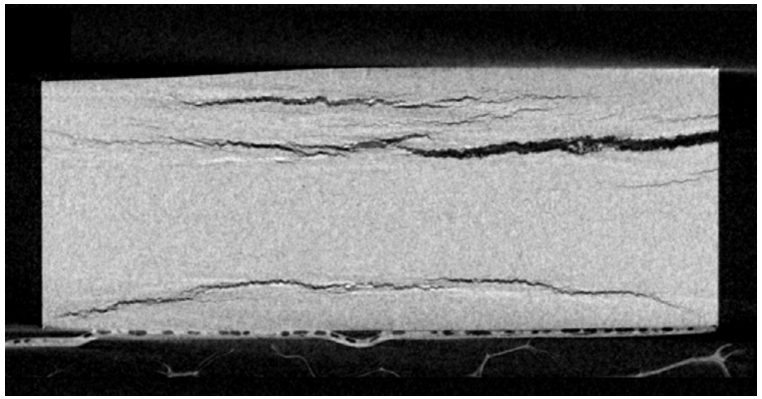

- MCC lamination defects observed under the following conditions:

- 200 mm/s punch velocity
- 285 MPa maximum axial stress
- Straight die
- Dwell times less than 100s

SRD Settings and Physical Consequences

Keyword	Value	Description
lamda	<not set>	Mean free path of SRD particles is automatically calculated through T_{SRD}.
collision	<noslip>	Collisions impart force and torque on big particles.
overlap	<yes>	Big particles are allowed to overlap.
inside	<ignore>	Do not flag an error when an SRD particle ends up in a big particle.
exact	<not set>	Automatically set to yes since overlap is yes, for time-accurate collisions.
radius	<0 to 1>	Scales down collision radius to avoid SRD particles colliding with multiple big particles.
bounce	<integer>	Maximum number of collisions an SRD particle can undergo in one timestep.
search	<not set>	Grid spacing for collision partner searching is set to hgrid.
cubic	<warn 0.0001>	Warning if bin size is non-cubic beyond specified tolerance.
shift	<yes 49829>	Bin shifting occurs each time SRD velocities are rescaled.
tstat	<yes>	SRD particles are thermostated to the specified temperature post-collision.
rescale	<yes>	SRD velocities are rescaled if particles travel more than four mean-free paths in one timestep.

Terminal Settling Velocity

$$\sum F = ma$$

$$F_d + F_b + F_g = ma$$

$$-6\pi\nu_a\rho_a Rv + \frac{4}{3}\pi R^3\rho_a g - \frac{4}{3}\pi R^3\rho_s g = \frac{4}{3}\pi R^3\rho_s\dot{v}$$

$$\dot{v} = c_1 v - c_2, \quad c_1 = -\frac{9}{2}\frac{\nu_a\rho_a}{R^2\rho_s}, \quad c_2 = \frac{\rho_a - \rho_s}{\rho_s}g$$

$$v(0) = 0 \rightarrow v = \frac{c_2}{c_1}(e^{c_1 t} - 1)$$

$$v_t = \frac{2}{9}\frac{(\rho_s - \rho_a)gR^2}{\nu_a\rho_a}$$

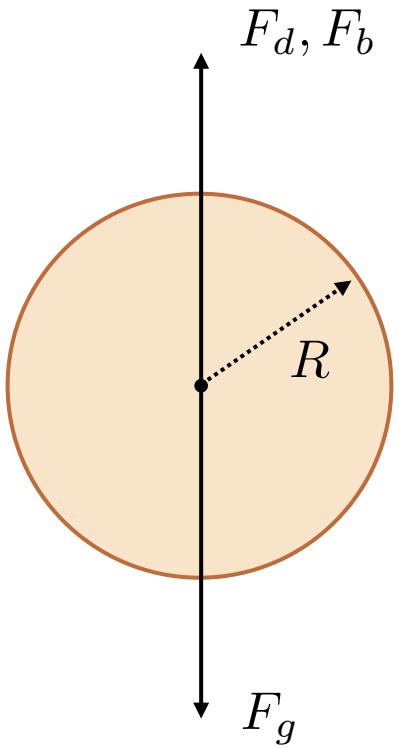

Drag, buoyant, and gravitational forces act on a spherical body as it falls through air.

Contact Area Scaling
(not dependent on radius)

$$A_T \propto N^2 A_i$$

$$A_i \propto R^2$$

$$R \propto \frac{L}{N}$$

$$A_i \propto \left(\frac{L}{N}\right)^2$$

$$A_T \propto L^2$$

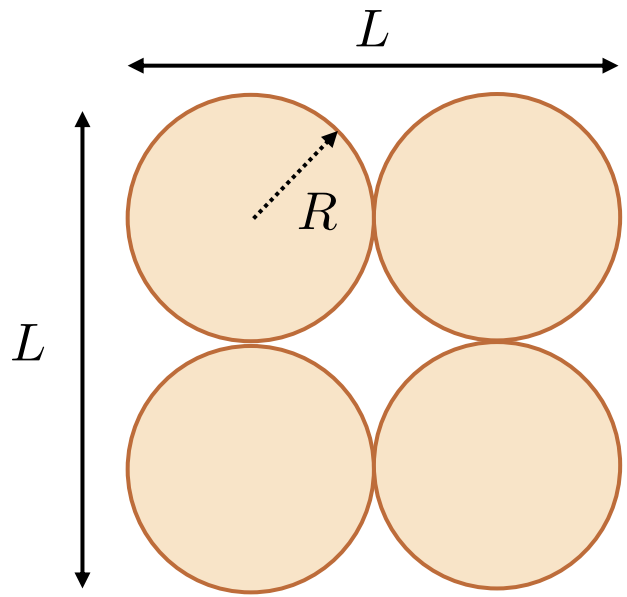

vs

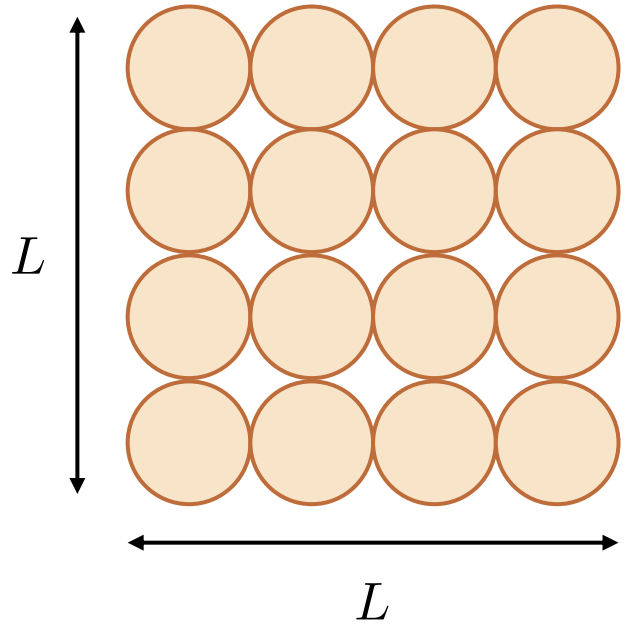

$R_1 = 2R_2$

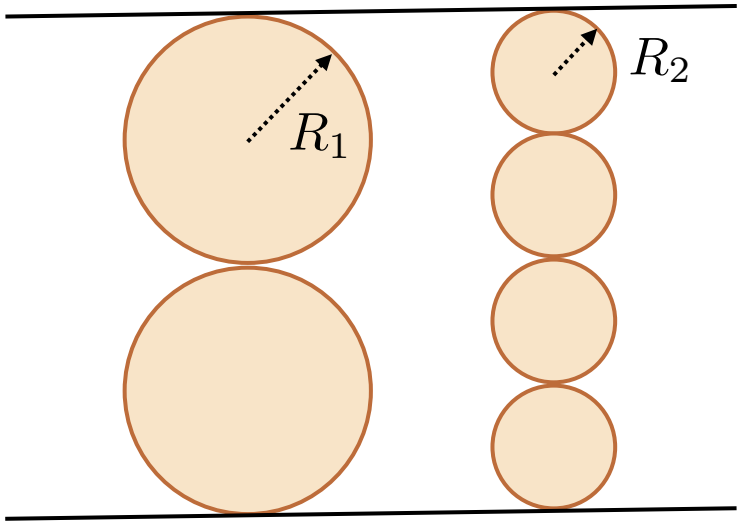

$\delta_1 = 2\delta_2$

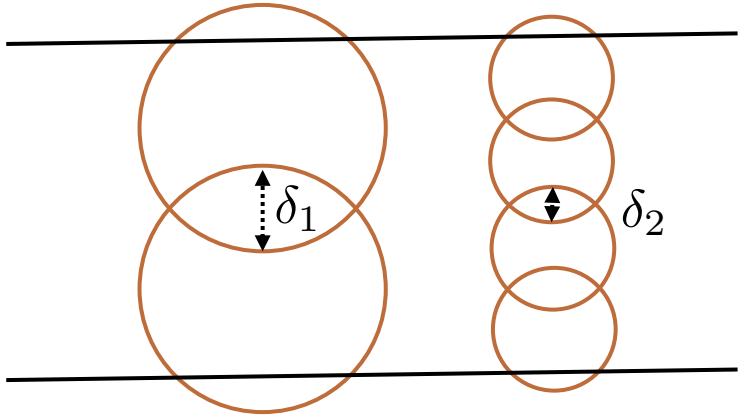

$$\delta \propto R$$

Hertz Peel-Off Stress and Energy

$$F_c \propto \Delta\gamma R$$

$$\sigma_c \propto \frac{\Delta\gamma}{R}$$

$$\delta_c \propto \left(\frac{\Delta\gamma^2 R}{E_c^*}\right)^{1/3}$$

$$U_{\text{adh}} \propto F_c \delta_c$$

$$U_{\text{adh}} \propto \frac{\Delta\gamma^{5/3} R^{4/3}}{(E_c^*)^{2/3}}$$

$$\frac{U_{\text{adh}}}{A} \propto \frac{\Delta\gamma^{5/3}}{(E_c^* R)^{2/3}}$$

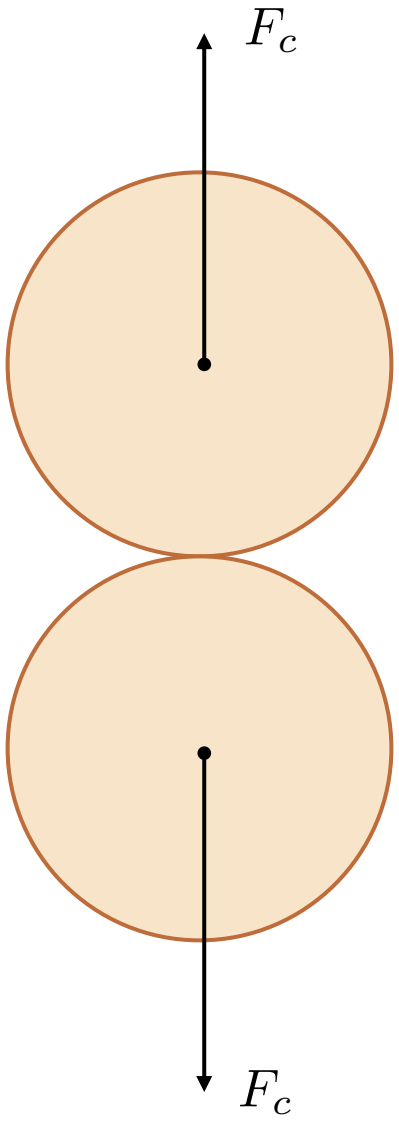

Force in adhesive bond

$$F_g + F_p + F_f + F_s = 0$$

$$F_g \propto \rho_s H L^2 g$$

$$F_p \propto P L^2$$

$$F_f \propto \mu_f \sigma_r H L$$

$$F_s \propto P L^2 - \rho_s H L^2 g - \mu_f \sigma_r H L$$

$$1e2 \text{ N} \qquad 1e-2 \text{ N} \qquad 1e2 \text{ N}$$

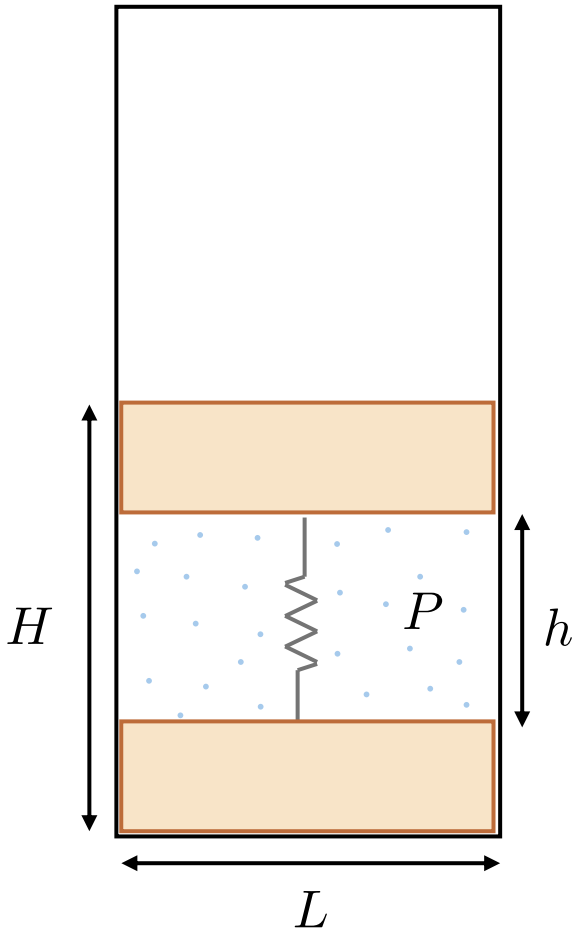

$$h \ll H$$

Terminal Settling Velocity

$$v_t \propto \frac{\rho_s g R^2}{\nu_a \rho_a}, \qquad \rho_s \gg \rho_a \qquad t_{\text{decay}} \propto \frac{\rho_s R^2}{\nu_a \rho_a}$$

Kozeny-Carman Equation

$$\frac{\Delta P}{L} \propto \frac{\nu_a \rho_a}{R^2} \frac{(1-\epsilon^2)}{\epsilon}$$

Gap flow-rate per unit length

$$q \propto \frac{w^3}{\nu_a \rho_a} \frac{\Delta P}{L}$$

Critical pull-off

$$\sigma_c \propto \frac{\gamma}{R} \qquad \frac{U_{\text{adh}}}{A} \propto \frac{\Delta \gamma^{5/3}}{(E_c^* R)^{2/3}}$$

Force in adhesive bond

$$F_s \propto PL^2 - \rho_s H L^2 g - \mu_f \sigma_r H L$$

$$\nu_{\mathrm{srd}}(a_{\mathrm{srd}}, \Delta t_{\mathrm{srd}}, M, \lambda) = \underbrace{\frac{a_{\mathrm{srd}}^2}{18\Delta t_{\mathrm{srd}}}\left[1 - \frac{1 - e^{-M}}{M}\right]}_{\nu_{\mathrm{coll}}} + \underbrace{\frac{\lambda^2}{4\Delta t_{\mathrm{srd}}}\frac{M+2}{M-1}}_{\nu_{\mathrm{kin}}}$$

a_{srd}	Bin size	free parameter but selecting a smaller value requires many more particles for $M > 1 \qquad (M \propto a_{\mathrm{srd}}^3)$
Δt_{srd}	Timestep between collisions	$\Delta t_{\mathrm{srd}} \geq \Delta t_{\mathrm{dem}}$
M	Average number of SRD particles per bin	$M = \frac{N_{\mathrm{srd}} a_{\mathrm{srd}}^3}{V_{\mathrm{srd}}}$ N_{srd} - Number of particles V_{srd} - Total volume
λ	Mean free path	$\lambda = \Delta t_{\mathrm{srd}} \sqrt{\frac{k_b T_{\mathrm{srd}}}{m_{\mathrm{srd}}}}$ k_b - Boltzmann constant T_{srd} - Temperature m_{srd} - Mass

$$\nu_{\text{srd}} = \frac{a_{\text{srd}}^2}{18\Delta t_{\text{srd}}}\left[1 - \frac{1-e^{-M}}{M}\right] + \frac{\lambda^2}{4\Delta t_{\text{srd}}}\frac{M+2}{M-1}$$

$M \geq 2 \qquad 0.56 \leq 1 - \dfrac{1-e^{-M}}{M} \leq 1$

$2 \leq M \leq 5 \qquad 1.75 \leq \dfrac{M+2}{M-1} \leq 4$

$2 \leq M \leq 5 \qquad \nu_{\text{srd}} \propto \dfrac{a_{\text{srd}}^2}{\Delta t_{\text{srd}}} + \dfrac{\lambda^2}{\Delta t_{\text{srd}}}$

$$\nu_{\text{srd}} = \frac{a_{\text{srd}}^2}{18\Delta t_{\text{srd}}}\left[1 - \frac{1-e^{-M}}{M}\right] + \frac{\Delta t_{\text{srd}} k_b T_{\text{srd}} M}{4a_{\text{srd}}^3 \rho_{\text{srd}}}\frac{M+2}{M-1}$$

$M \geq 2 \qquad 0.56 \leq 1 - \dfrac{1-e^{-M}}{M} \leq 1$

$2 \leq M \leq 5 \qquad 7.46 \leq M\dfrac{M+2}{M-1} \leq 8.75$

$2 \leq M \leq 5 \qquad \nu_{\text{srd}} \propto \dfrac{a_{\text{srd}}^2}{\Delta t_{\text{srd}}} + \dfrac{\Delta t_{\text{srd}} k_b T_{\text{srd}}}{a_{\text{srd}}^3 \rho_{\text{srd}}}$

Modeling Air Pressure

Zavalingos et al., 2017

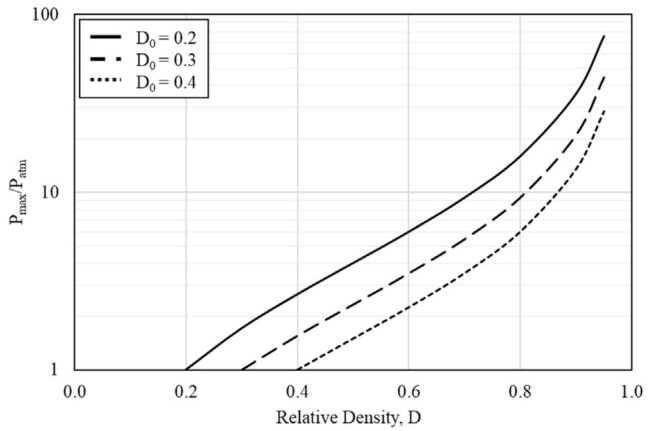

- Obtained 1D-approximate solution by combining gas phase mass continuity with D'Arcy's law.

- Important parameters for air pressure
  - Permeability
  - Compaction speed
  - Tablet size
  - Punch-die tolerance

Klinzing and Troup, 2019

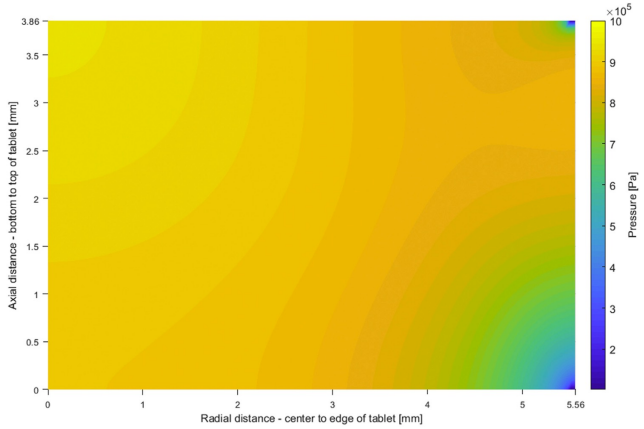

- 2D model with coupled air pressure and plasticity model for powder.

- Also observed similar 10-15x increased air pressure above 1 atm.